

# Detection of Freezing of Gait using Convolutional Neural Networks and Data from Lower Limb Motion Sensors

Bohan Shi<sup>1,2</sup>, Arthur Tay<sup>1</sup>, Dawn M.L. Tan<sup>3</sup>, Nicole S.Y. Chia<sup>4</sup>, W.L. Au<sup>4</sup>, and Shih-Cheng Yen<sup>5</sup>

**Abstract**—Parkinson's disease (PD) is a chronic, non-reversible neurodegenerative disorder, and freezing of gait (FOG) is one of the most disabling motor symptoms in PD, as it is often the leading cause of falls and injuries. In order to assess continuously and objectively PD patients who suffer from FOG and enable the possibility of on-demand cueing assistance, a sensor-based FOG detection solution can help clinicians manage the disease and help patients overcome freezing episodes. Many recent studies have leveraged deep learning models to detect FOG using signals extracted from accelerometers, gyroscopes, and magnetometers. Usually, the latent features and patterns of FOG are discovered from either the time or frequency domain. In this study, we investigated the use of the time-frequency domain by applying the continuous wavelet transform to signals from inertial measurement units placed on the lower limbs of 63 PD patients who suffered from FOG. We built convolutional neural networks to detect the FOG occurrences, and employed the Bayesian Optimisation approach to obtain the hyper-parameters. The results showed that the proposed subject-independent model was able to achieve a geometric mean of 90.7% and a F1 score of 91.5%.

## I. INTRODUCTION

PARKINSON'S disease (PD) is a progressive and non-reversible neurodegenerative disorder with predominantly motor impairments, such as tremor at rest, rigidity, bradykinesia, impairment of posture, and freezing of gait (FOG) [1]. Globally, PD affected about 6.1 million individuals in 2016 [2]. The estimates of the prevalence of PD range from 35.8 to 12,500 per 100,000 persons [3, 4]. The prevalence significantly increases with age, and studies have shown that the prevalence of PD for people above 65 years old is between 1.3% to 3% of that age group [5, 6]. Moreover, the number of patients diagnosed with PD increased by 31.6% from 2005 to 2015 [7], and the age-standardised prevalence of PD also increased by 21.7% from 1990 to 2016 [2]. PD is the fastest-growing

This work was supported in part by NUS-NNI 2016 Grant R263000C36133 and in part by NMRC/CISSP/2014/2015.

<sup>1</sup>B.H. Shi and A. Tay are with the Department of Electrical and Computer Engineering, National University of Singapore. Email: bohan.shi@u.nus.edu

<sup>2</sup>B.H. Shi is with Activate Interactive Pte. Ltd.

<sup>3</sup>D.M.L. Tan is with the Department of Physiotherapy, Singapore General Hospital.

<sup>4</sup>N.S.Y. Chia and W.L. Au are with the Department of Neurology, National Neuroscience Institute.

<sup>5</sup>S.-C. Yen is with the Innovation and Design Programme, Faculty of Engineering, National University of Singapore. Email: shihcheng@nus.edu.sg

neurological disease, and has become the most challenging health issue for ageing populations.

PD's pathological characteristics include the loss of dopaminergic neurons in the substantia nigra pars compacta and the accumulation of intracellular protein ( $\alpha$ -synuclein containing Lewy bodies) inside nerve cells that lead to cell death [8, 9]. The aetiology of PD is not well understood, but past studies have revealed a moderate correlation between PD causality and the role of environmental and genetic factors [10, 11]. The abnormal degeneration of dopaminergic neurons and the death of brain cells obstruct the smooth control and coordination of voluntary movements throughout the body. When 80% of dopamine-producing cells are damaged, the cardinal motor symptoms in PD start to emerge and significantly impair the performance of simple daily tasks such as walking and static standing. These motor impairments significantly reduce a patient's quality of life, but the most disabling motor symptom in PD is FOG, with half of all PD patients suffering the symptom [12, 13]. The clinical definition of FOG is "brief, episodic absence or marked reduction of forward progression of the feet despite the intention to walk" [14].

FOG usually happens to PD patients in the advanced stages, but a recent study has found that it could be found in the middle and late stages of PD [12]. It severely deteriorates PD subjects' mobility and restricts an individual's independence, often leading to falls, which are frequently associated with serious injuries. FOG is a paroxysmal and unpredictable motor anomaly, but some internal and external factors were found to induce a freezing episode, such as walking in a confined space, turning, dual-tasking, and stressful situations (e.g. inability to reach the destination) [15, 16]. FOG episodes usually continue for a few seconds, but can occasionally last for several minutes [17].

The primary symptomatic treatment for FOG is medication, and the most widely used medication is levodopa (L-dopa) therapy, which has demonstrated a positive effect on improving the dopamine-responsive type of FOG [18, 19]. Other types of treatments that tackle motor symptoms have not shown significant evidence to improve FOG, such as botulinum toxin injections and amantadine [20, 21].

Surgical treatment, such as deep brain stimulation (DBS) in the subthalamic nucleus or the globus pallidus area, is another approach to ease the burden of FOG [22-24]. However, DBS is not suitable for all PD patients as it is a highly invasive treatment that carries all the risks of major brain surgery [25].

Aside from treatments aimed at reducing the onset of freezing, there are also different approaches to mediate the consequences of freezing. Cueing is a movement strategy technique that supplements medication in improving the overall functional mobility of patients by assisting patients with PD to overcome FOG episodes and prevent falls [20, 26, 27]. The cueing techniques can be achieved in the form of rhythmic auditory cueing, visual assistance cues, and sensory cues. The cueing techniques's neural mechanisms are not well understood, but studies have shown that the disruptions in sensory-motor interactions might cause deficits in internal cueing for movements and movement initiation [28, 29]. The role that external cueing plays is to bypass the dysfunctional basal ganglia network and compensate for the loss of internal rhythms that results in impaired automaticity [30].

In order to deliver on-demand cueing assistance to PD patients at the most opportune moment to overcome the gait disturbance, wearable devices/systems have been proposed to monitor gait performance continuously and detect FOG events [31-33]. Technological advancements in wearable devices with small form factor single-board computers have made such a system feasible in recent years. Currently, the majority of studies have chosen to use inertial measurement unit (IMU) sensors (accelerometer and/or gyroscope) as they provide relatively accurate measurements and can be worn by patients for an extended period time without interrupting the walking pattern and normal activities of daily living. Other physiological wearable sensors, such as blood pressure and heart rate sensors and those that measure electrocardiograms and electromyograms, were also used in some studies to identify the physiological changes before the onset of FOG [?, 34]. Another way of detecting FOG is to use vision-based techniques to determine gait abnormalities [35, 36]. However, the results of vision-based methods have so far been worse than those of IMU-based approaches. The privacy and the security of the videos will also raise barriers to the adoption of these approaches.

In order to detect FOG events, conventional machine learning approaches have required a substantial amount of domain-related expertise and tremendous efforts in pre-processing and feature engineering on the data. However, no single feature or a combination of features have been shown to detect freezing episode perfectly due to the symptom's complexity and heterogeneity. Hence, researchers have recently started to adopt deep learning (DL) models to detect FOG without generating handcrafted features. Instead, the DL models were used to learn the features of the sensor data. Convolutional neural networks (CNN) are a type of neural network in DL, and they are the most popular model architecture for image classification. In recent years, its practical usage has extended from identifying objects from daily life, such as dogs and cats, to discovering symptoms, identifying diseases, and predicting biological structure [37-39]. In contrast to conventional machine learning approaches, CNN require minimum pre-processing, and they capture complex and heterogeneous features from data without extensive domain knowledge. It has naturally become a favoured tool to study clinical data.

In 2018, Camps et al. [40] introduced an 8-layer 1D CNN

to perform FOG detection. The model was trained using the REMPARK data set where 21 PD patients wore a nine-channel tri-axial IMU (accelerometer, gyroscope and magnetometer) on the left side of the wrist area while performing several walking tests at home. The data collected was segmented into 2.56 seconds windows, and every window of data was transformed into the frequency domain using the short-time Fast Fourier Transform (FFT). The magnitude of each FFT window was combined with the previous window of FFT data to form a single sample. The authors further processed the data with data augmentation in order to address the data imbalance issue. The model outperformed the previous shallow ML models and achieved 91.9% sensitivity, 89.5% specificity and 90.6% geometric mean.

Later that year, Xia et al. [41] presented a simpler 5-layer CNN. The data was collected from ten subjects with accelerometers placed on three different parts of their bodies. Outlier removal and data segmentation were performed, and the raw accelerometer data with a window size of four seconds was used as the model's input. The proposed CNN model was tested with two schemes. The patient-dependent model was able to detect FOG with an accuracy of 99%. The patient-independent model was trained using the leave-one-patient-out validation and achieved an accuracy of 80.7%.

In 2020, Sigcha et al. [42] proposed to use a combination of CNN and a Long Short-Term Memory (CNN-LSTM) deep neural network model on data collected from one single accelerometer that was placed on the participant's wrist. The study involved 21 participants, and the data collection was conducted at the patients' home to increase the occurrence of the FOG episodes. The authors found that stacking three previous spectral windows on the current window as the input of the CNN-LSTM model provided the best result, and they achieved mean sensitivity, specificity, and geometric mean all equal to 87.1% using the leave-one-subject-out validation.

Inspired by the latest research in CNN models, we propose a novel FOG detection method using CNN. We explored the possibility of leveraging time-frequency representations as the input to the CNN. The model was then optimised using the sequential model-based Bayesian optimisation method. In order to evaluate the proposed model's performance, we compared the proposed model with some machine learning algorithms and several state-of-the-art DL models. The preliminary design and results that were reported in a previous conference paper [43] were also reconstructed and examined.

## II. MATERIALS AND METHODS

### A. Data

Sixty-seven PD subjects who suffered from different degrees of FOG in the past agreed to participate in our study. All subjects were selected during their regular check-up and recommended by their respective neurologists from the local hospitals. The study was approved by the SingHealth Centralised Institutional Review Board of Singapore on 28th September 2016 (CIRB Ref: 2016/2743).

Each subject was instructed to performed two types of walking tests. The first one was the standard 7-metre Timed-Up-and-Go (7mTUG) test, and each subject conducted the

Characteristics	PD patients (n = 63)
Age (Year)	69.35 ± 12.4
<b>Gender</b>	
Male	41 (65.08%)
Female	22 (34.92%)
<b>Duration of Disease (Years)</b>	6.21 ± 4.83
<b>FOG-Q Total Score</b>	13.56 ± 4.62
<b>Average 7m-TUG (Seconds)</b>	71.82 ± 77.43

TABLE I: Demographics of the subjects.

test three times along with a physiotherapist and several researchers. As mentioned in our previous research [43], FOG subjects often experience "white-coat syndrome" where they do not experience FOG when performing walking tests with their neurologists or physiotherapists in a hospital or a laboratory. In order to reduce this phenomenon, we asked the subjects to walk freely in the clinics for the second test in order to capture more occurrences of freezing. The subjects wore an IMU around the lateral malleolus area of each ankle, and a third IMU near the 7th cervical (C7) vertebra during both tests. However, the data from the third sensor was not used in the FOG detection model. The IMU data was then transmitted wirelessly over a Bluetooth connection and saved into an iPad app at a sampling rate of 50 Hz.

Videos were recorded during the tests, and three experienced physiotherapists independently reviewed the videos after the tests in order to mark the FOG events. The final FOG labels were decided based on the decision of the majority. We ended up with a total of 431 FOG events in our database.

Within the sixty-seven subjects we recruited, data from four subjects who were unable to complete the tests, or encountered data loss during the tests, was excluded. Three subjects who suffered from FOG did not manifest any signs of freezing during the tests. Seven subjects demonstrated minimal or insignificant periods of FOG. However, recordings from these ten subjects were kept as examples of non-FOG gait. Four subjects faced significant challenges completing the test without walking aids, such as a walking frame or cane, so their data (which included periods of FOG) was collected with walking aids and used in our analyses. The rationale was that the use of walking aids in some environments was common in PD patients, so including this type of data would allow us to build a more robust system that could be used by PD patients to detect FOG in different environments.

The demographics of the sixty-three subjects who completed all the tests are shown in Table I.

## B. Signal Pre-Processing

1) *Data Filtering*: Signal pre-processing, such as filtering, is usually required for classification problems using time series data. However, DL models often require minimal filtering, and introducing noise into the input data is often used in

DL models to reduce generalisation error and improve model robustness [44]. Hence, in our experiments, the data was not filtered at all when training the CNN model.

When testing with the other machine learning models, the accelerometer signals were filtered with a 4th-order Butterworth band-pass filter. The cut-off frequencies were 0.2 Hz and 15 Hz. A 4th-order Butterworth low-pass filter was applied to the gyroscope signal with a cut-off frequency of 10 Hz. No pre-processing was performed on the magnetometer signals.

2) *Continuous Wavelet Transform*: Previous DL FOG detection algorithms used either the time domain raw data or frequency components obtained from the Fast Fourier transform (FFT). Time domain features, such as cadence and gait cycle duration, etc. have been shown to be effective in detecting FOG [45, 46]. Frequency domain features, such as power in the freezing band (3 to 8 Hz) and locomotor band (0.5 to 3 Hz), have also been shown to be sensitive predictors in FOG detection, and can be only discovered in the frequency domain. For example, Figure 1a shows non-FOG gait data from one of our subjects reflected in the orderly and periodic changes in the vertical axis of both the accelerometer and gyroscope signals. Figure 1b shows that most of the frequency components were distributed below 3 Hz. Figure 2a shows gait data from another one of our PD subjects suffering from a FOG episode. The data from the vertical axis of the accelerometer and gyroscope were much more random and distorted. Figure 2b shows that most of the frequency components were distributed between 3 Hz to 8 Hz.

However, based on observations of our own data and the results of past studies [33, 47], these patterns in the time or frequency domains were not always distinguishable for all patients. For the same patient, his/her FOG patterns also varied over time. This heterogeneity complicates the autonomous detection of FOG. Therefore, applying either raw time-domain data or transformed FFT data as the inputs for a CNN model can potentially lead to some critical features missing from the analysis and classification. This motivated us to make use of the wavelet transform, which would capture patterns in the time-frequency domain, to provide richer inputs to the CNN model. In Figure 1c and Figure 2c, data in the same window was transformed into the time-frequency plane using a continuous wavelet transform (CWT). The scalograms contained all the key information from the time and frequency domain analyses. Furthermore, they provided considerable additional insights into the non-stationarity of the IMU signals and the time specificity of power increases in different frequency bands.

As the CWT can provide a finer discretised scale for analysis than the discrete wavelet transform, we used the absolute value of the coefficients obtained from the Morlet CWT as the input to our CNN model. The mathematical representation of the CWT for a time-series data  $x(t)$  with respect to a mother wavelet  $\psi$ , is defined as :

$$CWT(s, \tau, \psi) = \int_{-\text{inf}}^{\text{inf}} x(t) \frac{1}{\sqrt{s}} \psi^* \left( \frac{t - \tau}{s} \right) dt, s \in R^{+*}, \tau \in R \quad (1)$$

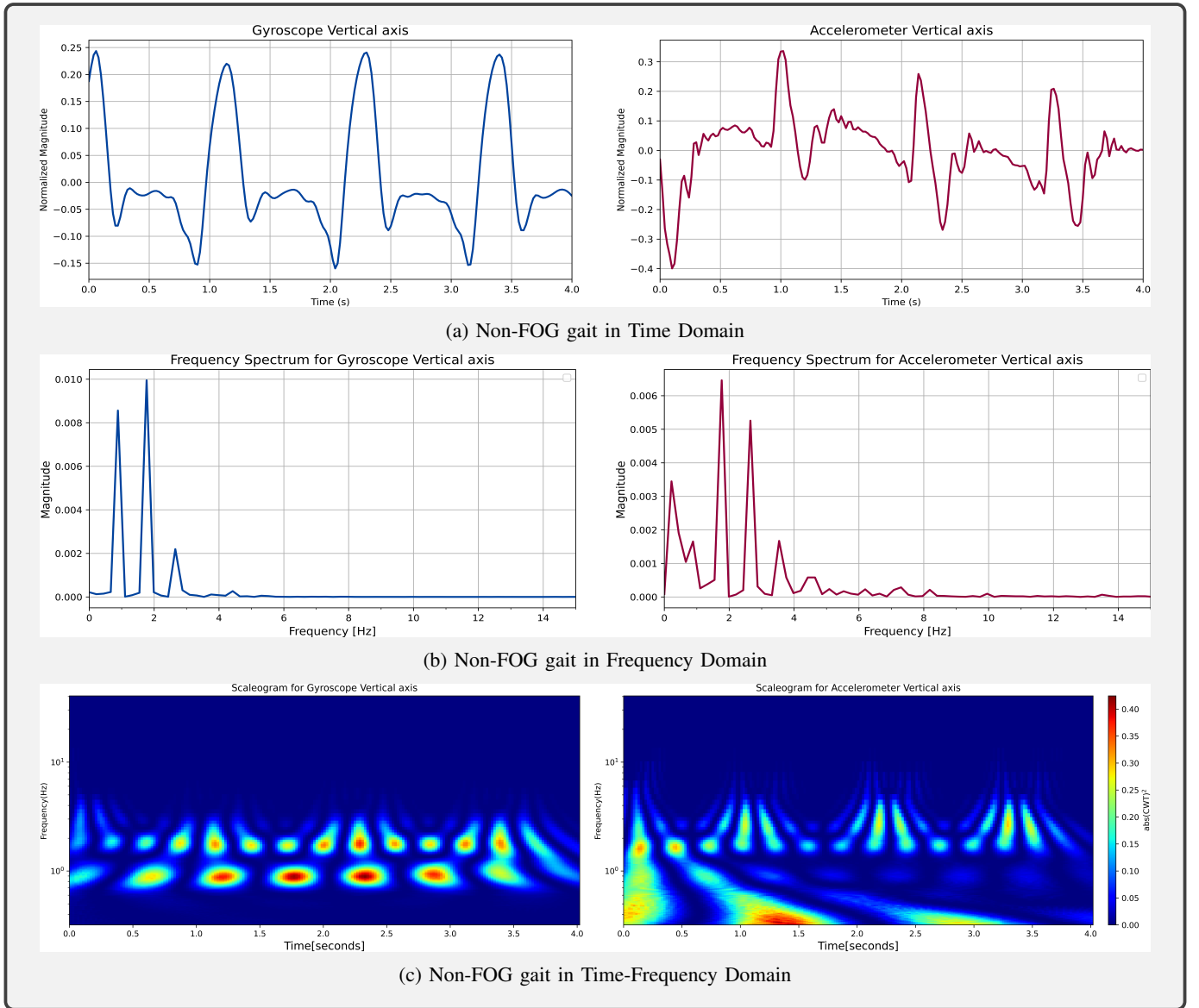


Fig. 1: Non-FOG gait signals visualised in time, frequency, and time-frequency domains.

where  $s$  and  $\tau$  are the scale and translation factors, respectively, used to transform the mother wavelet  $\psi$ , and  $*$  denotes the complex conjugate.

### C. Machine Learning Models

In order to compare the performance of DL models to machine learning models, 67 features that had been used in past FOG detection studies (described below) were trained using seven popular machine learning models. The features were extracted from the data in 1-second windows.

1) *Frequency Domain Features*: Moore et al. [48] and Delval et al. [45] pointed out that freezing of gait often occurred in the range of 3 to 8 Hz in the frequency spectra for vertical leg acceleration, while normal gait happened in the 0.5 to 3 Hz range. Therefore, we selected five widely used frequency domain features described in Table II.

Feature Name	Feature Description
Freeze Index (FI)	Power ratio in the freezing band (3 – 8 Hz) and the locomotor band (0.5 – 3 Hz) .
Total Power	Total power in the freezing band and the locomotor band.
Average Acceleration Energy	Average energy for all three axes of acceleration.
Sum of PSD	Sum of the power spectral density for vertical acceleration.
Peak Frequency	Peak frequency component for vertical acceleration.

TABLE II: Short descriptions of the selected frequency domain features for FOG detection.

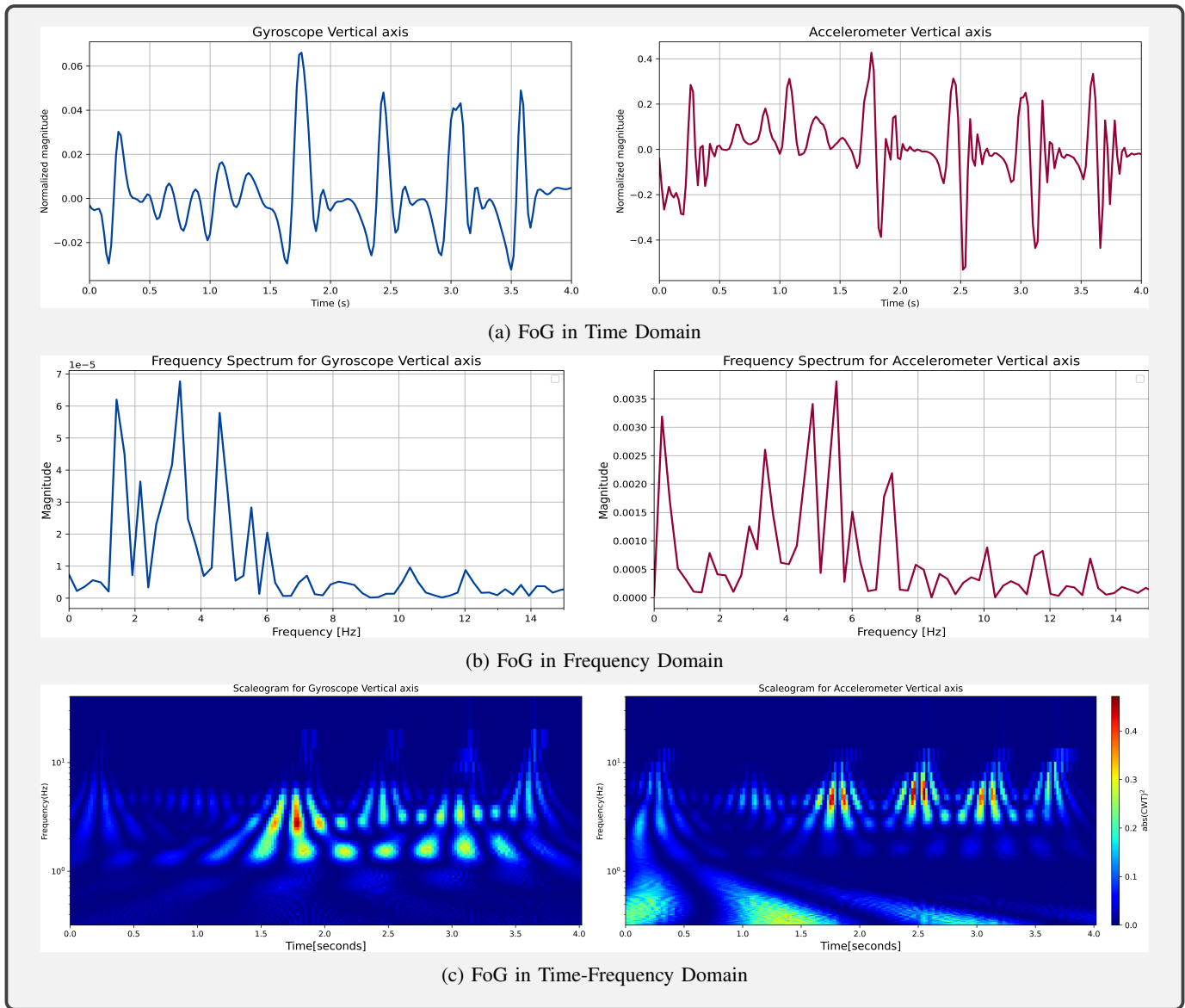


Fig. 2: FOG signals visualised in time, frequency, and time-frequency domains.

**2) Entropy Features:** Sample Entropy (SampEn) is an improved version of approximate entropy and is often used to evaluate a time-series data's complexity or regularity [49]. Human gait is a form of a dynamical system, and FOG is a sudden and episodic abnormality in the gait system [50, 51]. SampEn can be an effective method to analyse the regularity or stability of human gait where a higher SampEn value indicates a higher level of irregularity or randomness.

Sample Entropy calculation was performed for both accelerometer and gyroscope signals in the X, Y, and Z axes, as well as the signals' magnitudes. This feature extraction process was performed for each window of data to form the feature vector.

**3) Wavelet Features:** The wavelet transform is another popular method to analyse time-series signals. For example, El-Attar et al. [52] demonstrated that features extracted from applying discrete wavelet transform (DWT) on accelerometer

signals yielded a robust FOG classification model.

Therefore, we analysed the accelerometer signals using Daubechies orthogonal wavelets (db1) to extract the approximation (cA) and detail coefficients (cD) from the X, Y, and Z axes, as well as the magnitudes of the signals. Statistical features of the cA and cD, such as mean ( $\mu$ ), standard deviation ( $\sigma$ ), median, skewness (skew), kurtosis (kurt), minimum (min), maximum (max), interquartile range (iqr), and median absolute deviation (MAD) were calculated for 1 second of the data to form the wavelet feature vector.

#### D. Deep Learning Model Architecture

Extensive research on CNN has shown that models can learn more complex features as it goes deeper. However, training a deeper model is challenging as it requires a large amount of computational resources and data. Therefore, we limited our

network to a maximum of 8 CNN layers. An overview of the CNN architecture used is shown in Figure 3.

The first two CNN layers in the first 2D convolutional block contained 77 and 685 filters, respectively, and the kernel size was  $7 \times 7$ . A max-pooling layer with pool size of  $5 \times 5$  and stride size of  $2 \times 2$  was added after the CNN layer. The two CNN layers in the second and third blocks had identical configurations, except 128 filters were used in the second block and 464 filters were used in the third block. The kernel size in these two blocks was reduced to  $5 \times 5$ . The last block used a smaller  $3 \times 3$  kernel and 101 filters. A 2D global average pooling layer, followed by a fully connected layer with 512 neurons, was added at the end of the convolutional block. After the fully connected layer, a sigmoid activation function was used to determine the output. All convolutional blocks ended with a batch normalisation layer, a softsign activation layer, and a dropout layer. The dropout rate was set to 0.4.

We also used the following DL techniques in the model to improve model robustness and prevent overfitting:

1) *Regularization*: Overfitting is a common modelling issue, and it often occurs with CNN models. This error happens when the model fits the training data too well but fails to generalise to the test data. A few regularisation techniques to overcome overfitting were implemented in our model.

A large weight in CNNs will typically amplify noise in the input data, causing the error to increase further while propagating through the network. Hence, it is often an indicator of overfitting. Maximum normalised weight constraints were applied to all our convolution layers to ensure that the magnitude of weights did not exceed a given threshold during training.

A dropout layer is another regularisation technique to prevent overfitting. It randomly sets the output of some hidden neurons to zero during training at the given retaining probability. Dropout layers typically work well with a maximum normalised weight constraint. We tested different combinations of values for the maximum normalised weight and the dropout probability of retention, and the optimal result is discussed in the next section.

Early stopping was another regularisation method we used to prevent overfitting, where training was stopped when there were no significant decreases in validation loss over 20 epochs.

2) *Global Average Pooling*: Another technique used to reduce overfitting was introduced by Lin et al. [53] who introduced a global average pooling layer to replace the fully connected layer and enhance model discriminability within the receptive fields. Our model used a 2D global average pooling layer, followed by a fully connected layer at the end of the layer. The implementation has been used in recent advanced CNN architectures, such as EfficientNet [54] and MobileNet [55], as it reduces the computational cost of using two fully connected layers and maintains the performance of the model at the same time.

3) *Batch Normalisation*: Recent deep learning models have tended to increase their depth with multiple layers that are combined sequentially, with the inputs to each neural network layer coming from the activity of the previous layer. During the training process, the parameters in each neural layer will

be updated with each mini-batch of data, and this change of parameters will create a constant shift in the distribution of inputs [56, 57]. When these inputs propagate through the network, this small distribution change is amplified and causes a slowdown in the network convergence. This phenomenon has been described as an internal covariate shift [56]. We used batch normalisation in our network to normalise each layer's inputs to reduce the training time and improve the model's robustness [58].

### E. Model Optimisation

With the thousands of combinations of all the hyper-parameters, it would have been very time-consuming to identify the optimal hyper-parameters if we used the entire dataset. As such, we used only 30% of the data to search for the potential candidates and obtained an estimate of the optimal model performance. Furthermore, as the network structure was relatively complex, conventional hyper-parameter tuning approaches, such as the exhaustive grid search or random search, could not be performed using the full scale of the network as the computational cost would have been enormous. Hence, we adopted the "Taking the Human Out of the Loop" concept [59] and chose the Bayesian Optimisation approach to select the optimal combination of hyper-parameters, such as activation functions, dropout rate, kernel initialisers, weight constraints, optimisers, loss functions, and the number of filters in each layer. A hyper-parameter tuning library, scikit-optimize [60], was adopted in the fine-tuning process, and the Gradient Boosted Regression Trees technique was used to minimise the negative G-mean.

To speed up the fine-tuning process further, the model was trained using synchronous distributed training where each GPU ran a replica model with a local batch size of 10. We trained each combination of parameters for 50 epochs with a global batch size of 80 (the local batch size \* the number of GPUs). Theoretically, this training strategy would have increased the training speed by eight times.

We then set the total number of evaluations to 256, whereby the Bayesian Optimisation function drew 256 samples from the given options (shown in Table III) and tried to improve the validation G-mean over each iteration. The surrogate model used during this optimisation process was Gradient Boosted Regression Trees and the acquisition function was Expected Improvement (EI). However, there were no significant improvements after 154 evaluations, and the sequential optimisation process converged to a local minimum. The final set of hyper-parameters are summarised in Table III.

## III. RESULTS AND DISCUSSION

All experiments were conducted using Python, Tensorflow, and other relevant python libraries. The model was trained on an Nvidia Tesla V100 GPU using an Amazon Web Services Elastic Compute Cloud (EC2) cluster.

The data was split into 80% training data and 20% test data, i.e., 50 subjects in the training dataset and 13 subjects in the test dataset. During the training and validation process, the 10-fold cross-validation was performed using only the training data, and the test set was held out for final evaluation.

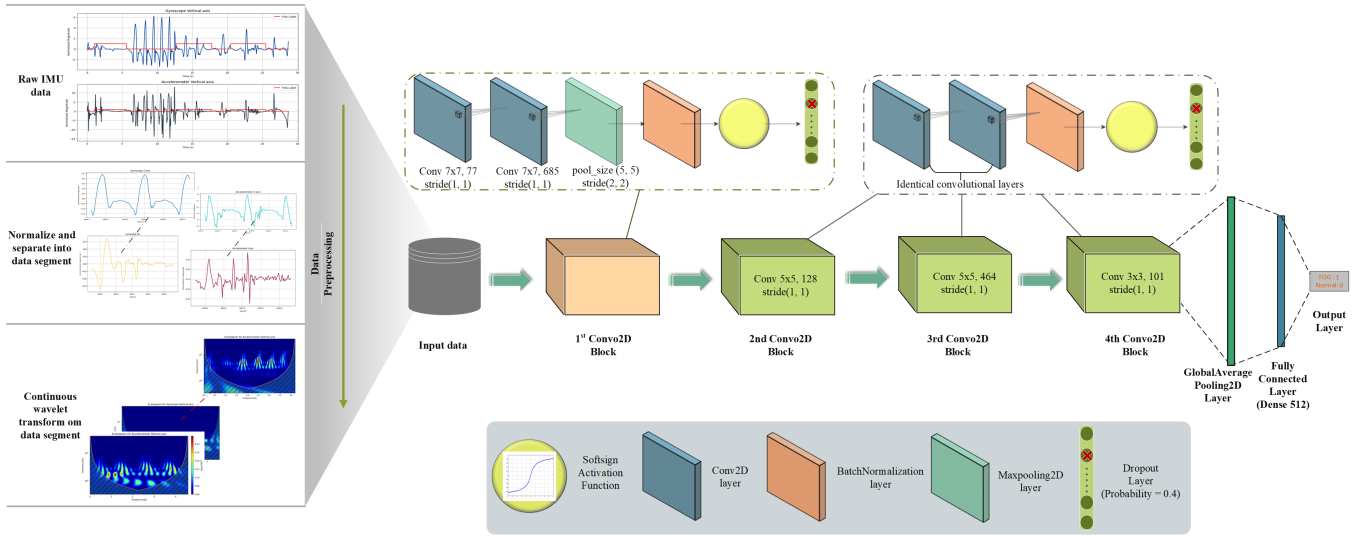


Fig. 3: Proposed CNN architecture.

Parameter	Options	Optimal Parameters
Activation Function	<ol style="list-style-type: none"> <li>relu</li> <li>softplus</li> <li>softsign</li> <li>selu</li> <li>swish</li> </ol>	softsign
Dropout Rate	$U(0.1, 0.9)$	0.4
Kernel Initializer	<ol style="list-style-type: none"> <li>lecun uniform</li> <li>lecun normal</li> <li>normal</li> <li>glorot normal</li> <li>glorot uniform</li> <li>he normal</li> <li>he uniform</li> <li>orthogonal</li> <li>variance scaling</li> </ol>	normal
Layer Weight Constraint	logU (0.6, 5)	1.8
Optimizer	<ol style="list-style-type: none"> <li>SGD</li> <li>RMSprop</li> <li>Adagrad</li> <li>Adadelta</li> <li>Adam</li> <li>Adamax</li> <li>Nadam</li> <li>Ftrl</li> </ol>	Adamax
Loss Function	<ol style="list-style-type: none"> <li>binary crossentropy</li> <li>sparse categorical crossentropy</li> <li>hinge</li> <li>squared hinge</li> </ol>	binary crossentropy

TABLE III: CNN hyperparameters explored using Bayesian Optimisation and the optimal parameters obtained.

### A. Data segmentation

The nine channels of IMU data were first fit with the training data to estimate the range of values and then normalised using the robust scaler transform. The normalised data were then segmented into smaller 4-second windows (200 samples), with a 50% overlap.

In similar studies, a window was labelled as a FOG window when all data in that window were FOG data [40], or more than 50% of the data in that window were FOG data [41]. However, in our data, a window that contained more than 0.2-second of FOG data (10% of the new information in each window, e.g. ten samples ) was labelled as a FOG window. The label of each window was determined using only the non-overlapping part of the data. The shortest FOG episode in our dataset was 0.04 seconds, which was the duration of a two frames in the videos used by the therapists to identify FOG. There were only 6 FOG episodes (1.2%) shorter than 0.2 seconds, and these episodes might not be detectable in real life. The rationale for labelling 0.2 seconds of FOG data as a FOG window was to minimise the detection latency and improve the detection robustness by training the model to recognise partial FOG windows and short FOG episodes. However, the obvious drawback is that the model's performance will deteriorate with this approach, which might be part of the reasons why the reconstructed models in this paper exhibited reduced performance.

### B. Model Evaluation

Six evaluation metrics were used to evaluate the proposed model's performance and compare it to other state-of-the-art algorithms Table IV. The Shapiro-Wilk normality test was performed on all evaluation metrics from all classification models. The one-tailed Student's t-test ( $\alpha = 0.05$ ) was used to test for statistically significant improvements if the distributions from both evaluation metrics passed the normality test, and the Hedge's g was reported for the effect size estimation. Otherwise, statistical significance was assessed

Evaluation Metrics	Mathematical Expression	Explanation
Accuracy	$\frac{TP+TN}{TP+TN+FP+FN}$	The total percentage of correctly classified windows.
Sensitivity / Recall	$\frac{TP}{TP+FN}$	The true positive rate, which corresponded to the ratio of FOG windows that were correctly classified as FOG windows.
Specificity	$\frac{TN}{TN+FP}$	The true negative rate, which indicated the proportion of non-FOG windows that were correctly considered as non-FOG.
Precision	$\frac{TP}{TP+FP}$	The ratio of correctly classified FOG windows to the total proportion of classified FOG windows.
Geometric Mean	$\sqrt[2]{Sensitivity * Specificity}$	The G-Mean, the square root of the product of the sensitivity and specificity, is a performance measurement that helps to balance the result among different classes.
F1-Score	$2 * \frac{Precision * Recall}{Precision + Recall}$	The harmonic mean of precision and recall is a evaluation metric that assesses the classification performance by evenly weighting recall and precision.

**TABLE IV:** Classification Evaluation Metrics. The true positive rate ( $TP$ ) indicated the proportion of FOG episodes correctly classified. The false positive rate ( $FP$ ) showed the proportion of non-FOG data windows misclassified as FOG episodes. The true negative rate ( $TN$ ) computed the proportion of non-FOG episodes that were classified accurately. The false-negative rate ( $FN$ ) was the proportion of FOG episodes misclassified as non-FOG episodes.

using the nonparametric Mann–Whitney U test ( $\alpha = 0.05$ ) and the Rank-Biserial Correlation was applied to determine the effect size.

For most PD patients, FOG events constitute only a small part of their regular walking experience. The gait data collected for FOG studies will always be imbalanced with FOG incidents being the minority class. We used the geometric mean (G-mean) and F1 score (harmonic mean of the precision and recall) as they are generally the most popular metrics used to evaluate model performance when taking into account data imbalances.

### C. Classification Result using ML Approach

Seven popular machine learning models were selected to evaluate the classification performance using conventional handcrafted features. All models were fine-tuned using a grid search to determine the best set of hyper-parameters. Each model was trained with Stratified 10-fold validation. The mean performance of models over the 10-fold validation is shown in Figure 4. The Extreme Gradient Boosting (XGBoost) showed the best performance in accuracy (80.65%), G-mean (81.03%), and F1 score (77.41%). Other models showed a mean classification accuracy below 80%. The XGBoost model also exhibited statistical improvement over KNN and SVM (radial basis kernel) models for several evaluation metrics, with effect sizes (Hedge’s  $g$ ) above 0.8 (Figure 4).

### D. Deep Learning Models Results

1) *Baseline CNN Model and Reconstructed Models:* We used our previously presented model [43] and re-trained the model with 10-fold cross-validation to evaluate the model performance. Furthermore, we reconstructed some of the state-of-the-art models mentioned in the first section as a comparison.

As the dataset was different, and because of the increased heterogeneity that existed in our data, the reconstructed model did not achieve the performance reported in the original articles. The result is shown in Figure 5.

2) *Proposed CNN Model:* We trained the models with a 10-fold cross-validation scheme and evaluated them with the hold-out test set to demonstrate that the proposed CNN model outperformed previous models. Figure 5 shows that the proposed CNN model exhibited a statistically significant improvement from the ML models for the average accuracy, precision, G-mean, and F1 score. All metrics except the sensitivity were significantly improved compared to Xia’s model. However, the proposed model displayed significant improvements from Camps’s model only in specificity, precision, and G-mean. The average accuracy, specificity, G-mean, and F1 score were also significantly improved from the CNN baseline model. All the significant improvements in the metrics showed substantial effect size (Hedge’s  $g > 0.8$  or the Rank-Biserial correlation  $> 0.5$ ), indicating large practical differences [61, 62]. The only three exceptions were when the CNN baseline model’s F1 score was compared with the best ML model, and the proposed model’s F1 score was compared with the F1 scores from the CNN baseline model and Xia’s model. These metrics failed the normality test, and the correlation was below 0.5. Furthermore, the proposed model showed significant improvement over G-mean against all the models with substantial effect size.

The best performance obtained from the proposed model achieved a 90.7% G-mean and 91.5% F1 score. Furthermore, the proposed model and the reconstructed Camps’s model displayed minor performance fluctuations throughout the 10-fold cross-validation, indicating that these two models provided similar performance levels with data from new subjects. No significant improvement for sensitivity was found in the statistical analysis, mainly because the proposed model was optimised to find the best G-mean performance.

## IV. CONCLUSION

In the last two decades, FOG detection algorithms have slowly changed from classical feature extraction and statistical analysis methods toward adopting various machine learning (ML) and deep learning (DL) algorithms and techniques to discover data characteristics. However, FOG detection still remains a challenging problem because of the complexity and heterogeneity of the symptoms. Another challenge is the amount of high-quality data available to develop a reliable and robust deep learning model.

In this study, we proposed a novel method to analyse IMU data using time-frequency analysis and proposed a robust model structure that was trained and validated on a relatively large cohort of PD patients who suffered from FOG. Using the "Taking the Human Out of the Loop" concept, we employed Bayesian Optimisation to determine the optimal hyperparameters and the final model design. Our proposed design is also a subject-independent model, and it is immune to the fluctuation in gait patterns when PD patient mobility deteriorates over time. The empirical results also indicated that the model can provide consistent performance and excellent FOG detection

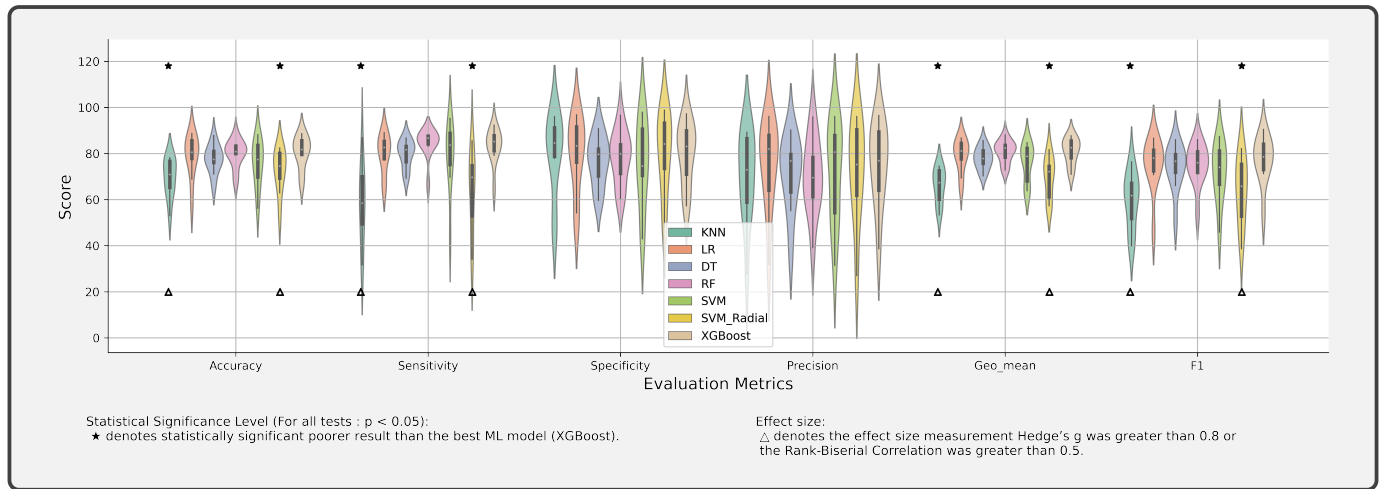


Fig. 4: ML classification results with the selected FOG features.

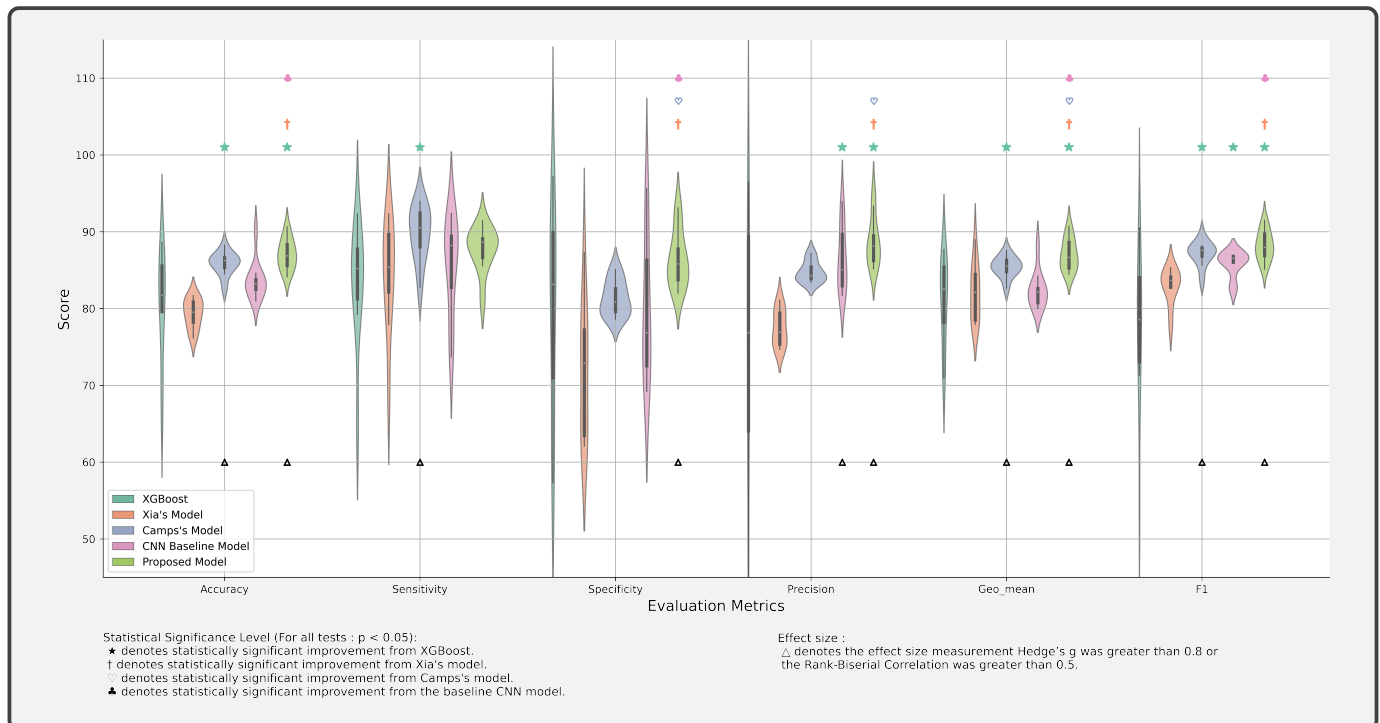


Fig. 5: Classification performance for the baseline and re-constructed models.

accuracy. Moreover, the statistically significant improvement of G-mean in the proposed model compared against all other models demonstrated that the Bayesian optimisation approach could effectively determine the hyperparameter over desired evaluation metrics or objective functions. However, the proposed model used time-frequency representations as inputs, and this makes the model similar to a computer vision solution. Hence, the main limitations of this model are that the model does not reduce the computational cost, and it relies heavily on GPUs to process the data.

## REFERENCES

- [1] L. V. Kalia and A. E. Lang, "Parkinson's disease," *The Lancet*, vol. 386, no. 9996, pp. 896–912, aug 2015.
- [2] GBD 2016 Parkinson's Disease Collaborators, "Global, regional, and national burden of Parkinson's disease, 1990–2016: a systematic analysis for the Global Burden of Disease Study 2016." *The Lancet. Neurology*, vol. 17, no. 11, pp. 939–953, nov 2018.
- [3] S. Von Campenhausen, B. Bornschein, R. Wick, K. Bötzel, C. Sampaio, W. Poewe, W. Oertel, U. Siebert, K. Berger, and R. Dodel, "Prevalence and incidence of Parkinson's disease in Europe," *European Neuropsychopharmacology*, vol. 15, no. 4, pp. 473–490, aug 2005.
- [4] W. Muangpaisan, H. Hori, and C. Brayne, "Systematic review of the prevalence and incidence of Parkinson's disease in Asia," *Journal of Epidemiology*, vol. 19, no. 6, pp. 281–293, 2009.
- [5] O. Riedel, D. Bitters, U. Amann, E. Garbe, and I. Langner, "Estimating the prevalence of Parkinson's disease (PD) and proportions of patients

- with associated dementia and depression among the older adults based on secondary claims data," *International Journal of Geriatric Psychiatry*, vol. 31, no. 8, pp. 938–943, aug 2016.
- [6] W. Poewe, K. Seppi, C. M. Tanner, G. M. Halliday, P. Brundin, J. Volkman, A. E. Schrag, and A. E. Lang, "Parkinson disease," *Nature Reviews Disease Primers*, vol. 3, pp. 1–21, mar 2017.
- [7] G. . P. D. Collaborators, "Global, regional, and national incidence, prevalence, and years lived with disability for 310 diseases and injuries, 1990–2015: a systematic analysis for the Global Burden of Disease Study 2015," *The Lancet*, vol. 388, no. 10053, pp. 1545–1602, oct 2016.
- [8] G. Alves, E. B. Forsaa, K. F. Pedersen, M. Dreetz Gjerstad, and J. P. Larsen, "Epidemiology of Parkinson's disease," *Journal of Neurology*, vol. 255, no. SUPPL. 5, pp. 18–32, sep 2008.
- [9] O. B. Tysnes and A. Storstein, "Epidemiology of Parkinson's disease," *Journal of Neural Transmission*, vol. 124, no. 8, pp. 901–905, aug 2017.
- [10] A. H. Schapira, "Etiology of Parkinson's disease," *Neurology*, vol. 66, no. Issue 10, Supplement 4, pp. S10–S23, may 2006.
- [11] K. Wirdefeldt, H. O. Adami, P. Cole, D. Trichopoulos, and J. Mandel, "Epidemiology and etiology of Parkinson's disease: A review of the evidence," *European Journal of Epidemiology*, vol. 26, no. SUPPL. 1, jun 2011.
- [12] N. Giladi, T. A. Treves, E. S. Simon, H. Shabtai, Y. Orlov, B. Kandinov, D. Paleacu, and A. D. Korczyn, "Freezing of gait in patients with advanced Parkinson's disease," *Journal of Neural Transmission*, vol. 108, no. 1, pp. 53–61, 2001.
- [13] N. Giladi, M. P. McDermott, S. Fahn, S. Przedborski, J. Jankovic, M. Stern, and C. Tanner, "Freezing of gait in PD: Prospective assessment in the DATATOP cohort," *Neurology*, vol. 56, no. 12, pp. 1712–1721, jun 2001.
- [14] J. G. Nutt, B. R. Bloem, N. Giladi, M. Hallett, F. B. Horak, and A. Nieuwboer, "Freezing of gait: Moving forward on a mysterious clinical phenomenon," *The Lancet Neurology*, vol. 10, no. 8, pp. 734–744, aug 2011.
- [15] A. Nieuwboer and N. Giladi, "The challenge of evaluating freezing of gait in patients with Parkinson's disease," *British Journal of Neurosurgery*, vol. 22, no. SUPPL. 1, pp. S16–S18, jan 2008.
- [16] Y. Okuma and N. Yanagisawa, "The clinical spectrum of freezing of gait in Parkinson's disease," *Movement Disorders*, vol. 23, no. SUPPL. 2, pp. S426–30, 2008.
- [17] A. H. Snijders, M. J. Nijkrake, M. Bakker, M. Munneke, C. Wind, and B. R. Bloem, "Clinimetrics of freezing of gait," *Movement Disorders*, vol. 23, no. SUPPL. 2, pp. S468–S474, 2008.
- [18] J. D. Schaafsma, Y. Balash, T. Gurevich, A. L. Bartels, J. M. Hausdorff, and N. Giladi, "Characterization of freezing of gait subtypes and the response of each to levodopa in Parkinson's disease," *European Journal of Neurology*, vol. 10, no. 4, pp. 391–398, jul 2003.
- [19] J. Lucas McKay, F. C. Goldstein, B. Sommerfeld, D. Bernhard, S. Perez Parra, and S. A. Factor, "Freezing of Gait can persist after an acute levodopa challenge in Parkinson's disease," *npj Parkinson's Disease*, vol. 5, no. 1, p. 25, dec 2019.
- [20] J. Nonnekes, A. H. Snijders, J. G. Nutt, G. Deuschl, N. Giladi, and B. R. Bloem, "Freezing of gait: A practical approach to management," *The Lancet Neurology*, vol. 14, no. 7, pp. 768–778, jul 2015.
- [21] L.-L. Zhang, S. Duff Canning, and X.-P. Wang, "Freezing of Gait in Parkinsonism and its Potential Drug Treatment," *Current Neuropharmacology*, vol. 14, no. 4, pp. 302–306, apr 2016.
- [22] G. Deuschl, C. Schade-Brittinger, P. Krack, J. Volkman, H. Schäfer, K. Bötzel, C. Daniels, A. Deuschländer, U. Dillmann, W. Eisner, D. Gruber, W. Hamel, J. Herzog, R. Hilker, S. Klebe, M. Kloß, J. Koy, M. Krause, A. Kupsch, D. Lorenz, S. Lorenzl, H. M. Mehdorn, J. H. Moringlane, W. Oertel, M. O. Pinsker, H. Reichmann, A. Reuß, G. R. Schneider, A. Schntzler, U. Steude, V. Sturm, L. Timmermann, V. Tronnier, T. Trottenberg, L. Wojtecki, E. Wolf, W. Poewe, and J. Voges, "A randomized trial of deep-brain stimulation for Parkinson's disease," *New England Journal of Medicine*, vol. 355, no. 9, pp. 896–908, aug 2006.
- [23] V. Ricchi, M. Zibetti, S. Angrisano, A. Merola, N. Arduino, C. A. Artusi, M. Rizzone, L. Lopiano, and M. Lanotte, "Transient effects of 80 Hz stimulation on gait in STN DBS treated PD patients: A 15 months follow-up study," *Brain Stimulation*, vol. 5, no. 3, pp. 388–392, jul 2012.
- [24] T. Xie, J. Vigil, E. MacCracken, A. Gasparaitis, J. Young, W. Kang, J. Bernard, P. Warnke, and U. J. Kang, "Low-frequency stimulation of STN-DBS reduces aspiration and freezing of gait in patients with PD," *Neurology*, vol. 84, no. 4, pp. 415–420, 2015.
- [25] T. B. Stoker, K. M. Torsney, and R. A. Barker, "Emerging treatment approaches for Parkinson's disease," *Frontiers in Neuroscience*, vol. 12, no. OCT, oct 2018.
- [26] L. Rochester, V. Hetherington, D. Jones, A. Nieuwboer, A. M. Willems, G. Kwakkel, and E. Van Wegen, "The effect of external rhythmic cues (auditory and visual) on walking during a functional task in homes of people with Parkinson's disease," *Archives of Physical Medicine and Rehabilitation*, vol. 86, no. 5, pp. 999–1006, may 2005.
- [27] M. E. Morris, C. L. Martin, and M. L. Schenkman, "Striding Out With Parkinson Disease: Evidence-Based Physical Therapy for Gait Disorders," *Physical Therapy*, vol. 90, no. 2, pp. 280–288, feb 2010.
- [28] A. Nieuwboer, "Cueing for freezing of gait in patients with Parkinson's disease: A rehabilitation perspective," *Movement Disorders*, vol. 23, no. S2, pp. S475–S481, jul 2008.
- [29] S. Ghai, I. Ghai, G. Schmitz, and A. O. Effenberg, "Effect of rhythmic auditory cueing on parkinsonian gait: A systematic review and meta-analysis," *Scientific Reports*, vol. 8, no. 1, p. 506, dec 2018.
- [30] S. J. Spaulding, B. Barber, M. Colby, B. Cormack, T. Mick, and M. E. Jenkins, "Cueing and Gait Improvement Among People With Parkinson's Disease: A Meta-Analysis," *Archives of Physical Medicine and Rehabilitation*, vol. 94, no. 3, pp. 562–570, mar 2013.
- [31] P. Ginis, E. Heremans, A. Ferrari, E. M. Bekkers, C. G. Canning, and A. Nieuwboer, "External input for gait in people with Parkinson's disease with and without freezing of gait: One size does not fit all," *Journal of Neurology*, vol. 264, no. 7, pp. 1488–1496, jul 2017.
- [32] M. Gilat, A. Lúcia Silva de Lima, B. R. Bloem, J. M. Shine, J. Nonnekes, and S. J. Lewis, "Freezing of gait: Promising avenues for future treatment," *Parkinsonism and Related Disorders*, vol. 52, pp. 7–16, jul 2018.
- [33] V. Mikos, C. H. Heng, A. Tay, S. C. Yen, N. S. Y. Chia, K. M. L. Koh, D. M. L. Tan, and W. L. Au, "A Wearable, Patient-Adaptive Freezing of Gait Detection System for Biofeedback Cueing in Parkinson's Disease," *IEEE Transactions on Biomedical Circuits and Systems*, vol. 13, no. 3, pp. 503–515, jun 2019.
- [34] A. Nieuwboer, R. Dom, W. De Weerd, K. Desloovere, S. Fieuws, and E. Broens-Kaucsik, "Abnormalities of the spatiotemporal characteristics of gait at the onset of freezing in Parkinson's disease," *Movement Disorders*, vol. 16, no. 6, pp. 1066–1075, nov 2001.
- [35] R. Sun, Z. Wang, K. E. Martens, and S. Lewis, "Convolutional 3D Attention Network for Video Based Freezing of Gait Recognition," in *2018 International Conference on Digital Image Computing: Techniques and Applications, DICTA 2018*. Institute of Electrical and Electronics Engineers Inc., jan 2019.
- [36] K. Hu, Z. Wang, S. Mei, K. A. Ehgoetz Martens, T. Yao, S. J. Lewis, and D. D. Feng, "Vision-Based Freezing of Gait Detection with Anatomic Directed Graph Representation," *IEEE Journal of Biomedical and Health Informatics*, vol. 24, no. 4, pp. 1215–1225, apr 2020.
- [37] R. Miotto, F. Wang, S. Wang, X. Jiang, and J. T. Dudley, "Deep learning for healthcare: Review, opportunities and challenges," *Briefings in Bioinformatics*, vol. 19, no. 6, pp. 1236–1246, nov 2017.
- [38] O. Faust, Y. Hagiwara, T. J. Hong, O. S. Lih, and U. R. Acharya, "Deep learning for healthcare applications based on physiological signals: A review," pp. 1–13, jul 2018.
- [39] A. W. Senior, R. Evans, J. Jumper, J. Kirkpatrick, L. Sifre, T. Green, C. Qin, A. Židek, A. W. Nelson, A. Bridgland, H. Penedones, S. Petersen, K. Simonyan, S. Crossan, P. Kohli, D. T. Jones, D. Silver, K. Kavukcuoglu, and D. Hassabis, "Improved protein structure prediction using potentials from deep learning," *Nature*, vol. 577, no. 7792, pp. 706–710, jan 2020.
- [40] J. Camps, A. Samà, M. Martín, D. Rodríguez-Martín, C. Pérez-López, J. M. Moreno Arostegui, J. Cabestany, A. Català, S. Alcaine, B. Mestre, A. Prats, M. C. Crespo-Maraver, T. J. Counihan, P. Browne, L. R. Quinlan, G. Ó. Laighin, D. Sweeney, H. Lewy, G. Vainstein, A. Costa, R. Annicchiarico, A. Bayés, and A. Rodríguez-Molinero, "Deep learning for freezing of gait detection in Parkinson's disease patients in their homes using a waist-worn inertial measurement unit," *Knowledge-Based Systems*, vol. 139, pp. 119–131, jan 2018.
- [41] Y. Xia, J. Zhang, Q. Ye, N. Cheng, Y. Lu, and D. Zhang, "Evaluation of deep convolutional neural networks for detection of freezing of gait in Parkinson's disease patients," *Biomedical Signal Processing and Control*, vol. 46, pp. 221–230, sep 2018.
- [42] L. Sigcha, N. Costa, I. Pavón, S. Costa, P. Arezes, J. M. López, and G. De Arcas, "Deep learning approaches for detecting freezing of gait in parkinson's disease patients through on-body acceleration sensors," *Sensors*, vol. 20, no. 7, p. 1895, mar 2020.
- [43] B. Shi, S. C. Yen, A. Tay, D. M. Tan, N. S. Chia, and W. L. Au, "Convolutional Neural Network for Freezing of Gait Detection Leveraging the Continuous Wavelet Transform on Lower Extremities Wearable Sensors Data," in *Proceedings of the Annual International Conference of the IEEE Engineering in Medicine and Biology Society*,

- EMBS*, vol. 2020-July. Institute of Electrical and Electronics Engineers Inc., jul 2020, pp. 5410–5415.
- [44] I. Goodfellow, Y. Bengio, and C. Aaron, “Dataset Augmentation,” in *Deep Learning*. MIT Press, 2016, ch. 7, p. 237.
- [45] A. Delval, A. H. Snijders, V. Weerdesteyn, J. E. Duysens, L. Defebvre, N. Giladi, and B. R. Bloem, “Objective detection of subtle freezing of gait episodes in Parkinson’s disease,” *Movement Disorders*, vol. 25, no. 11, pp. 1684–1693, aug 2010.
- [46] P. Tahafchi, R. Molina, J. A. Roper, K. Sowalsky, C. J. Hass, A. Gunduz, M. S. Okun, and J. W. Judy, “Freezing-of-Gait detection using temporal, spatial, and physiological features with a support-vector-machine classifier,” in *Proceedings of the Annual International Conference of the IEEE Engineering in Medicine and Biology Society, EMBS*. Institute of Electrical and Electronics Engineers Inc., sep 2017, pp. 2867–2870.
- [47] V. Mikos, C. H. Heng, A. Tay, N. S. Y. Chia, K. M. L. Koh, D. M. L. Tan, and W. L. Au, “Optimal window lengths, features and subsets thereof for freezing of gait classification,” in *ICIBMS 2017 - 2nd International Conference on Intelligent Informatics and Biomedical Sciences*, vol. 2018-Janua. Institute of Electrical and Electronics Engineers Inc., feb 2018, pp. 1–8.
- [48] S. T. Moore, H. G. MacDougall, and W. G. Ondo, “Ambulatory monitoring of freezing of gait in Parkinson’s disease,” *Journal of Neuroscience Methods*, vol. 167, no. 2, pp. 340–348, jan 2008.
- [49] J. S. Richman and J. R. Moorman, “Physiological time-series analysis using approximate and sample entropy,” *American Journal of Physiology - Heart and Circulatory Physiology*, vol. 278, no. 6 47-6, pp. 2039–2049, 2000.
- [50] J. M. Hausdorff, “Gait dynamics in Parkinson’s disease: Common and distinct behavior among stride length, gait variability, and fractal-like scaling,” *Chaos*, vol. 19, no. 2, 2009.
- [51] N. G. Pozzi, A. Canessa, C. Palmisano, J. Brumberg, F. Steigerwald, M. M. Reich, B. Minafra, C. Pacchetti, G. Pezzoli, J. Volkmann, and I. U. Isaias, “Freezing of gait in Parkinson’s disease reflects a sudden derangement of locomotor network dynamics,” *Brain*, vol. 142, no. 7, pp. 2037–2050, jul 2019.
- [52] A. El-Attar, A. S. Ashour, N. Dey, H. Abdelkader, M. M. Abd El-Naby, and R. S. Sherratt, “Discrete wavelet transform-based freezing of gait detection in Parkinson’s disease,” *Journal of Experimental and Theoretical Artificial Intelligence*, pp. 1–17, sep 2018.
- [53] M. Lin, Q. Chen, and S. Yan, “Network in network,” in *2nd International Conference on Learning Representations, ICLR 2014 - Conference Track Proceedings*, dec 2014.
- [54] M. Tan and Q. V. Le, “EfficientNet: Rethinking model scaling for convolutional neural networks,” in *36th International Conference on Machine Learning, ICML 2019*, vol. 2019-June. International Machine Learning Society (IMLS), may 2019, pp. 10 691–10 700.
- [55] A. Howard, M. Sandler, B. Chen, W. Wang, L. C. Chen, M. Tan, G. Chu, V. Vasudevan, Y. Zhu, R. Pang, Q. Le, and H. Adam, “Searching for mobileNetV3,” in *Proceedings of the IEEE International Conference on Computer Vision*, vol. 2019-October. Institute of Electrical and Electronics Engineers Inc., may 2019, pp. 1314–1324.
- [56] S. Ioffe and C. Szegedy, “Batch Normalization: Accelerating Deep Network Training by Reducing Internal Covariate Shift,” in *32nd International Conference on Machine Learning, ICML 2015*, vol. 1. International Machine Learning Society (IMLS), feb 2015, pp. 448–456.
- [57] S. Santurkar, D. Tsipras, A. Ilyas, and A. Madry, “How does batch normalization help optimization?” in *Advances in Neural Information Processing Systems*, vol. 2018-December, may 2018, pp. 2483–2493.
- [58] G. Yang, J. Pennington, V. Rao, J. Sohl-Dickstein, and S. S. Schoenholz, “A mean field theory of batch normalization,” in *7th International Conference on Learning Representations, ICLR 2019*. International Conference on Learning Representations, ICLR, feb 2019.
- [59] B. Shahriari, K. Swersky, Z. Wang, R. P. Adams, and N. De Freitas, “Taking the human out of the loop: A review of Bayesian optimization,” *Proceedings of the IEEE*, vol. 104, no. 1, pp. 148–175, jan 2016.
- [60] T. Head, M. Kumar, H. Nahrstaedt, G. Louppe, and I. Shcherbatyi, “scikit-optimize/scikit-optimize,” sep 2020.
- [61] C. J. Ferguson, “An effect size primer: A guide for clinicians and researchers,” in *Methodological issues and strategies in clinical research (4th ed.)*. Washington: American Psychological Association, dec 2015, pp. 301–310.
- [62] D. C. Funder and D. J. Ozer, “Evaluating Effect Size in Psychological Research: Sense and Nonsense,” *Advances in Methods and Practices in Psychological Science*, vol. 2, no. 2, pp. 156–168, jun 2019.